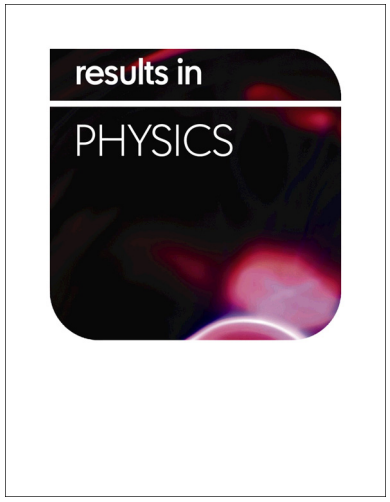

Structural And Electrical Properties Of Al_{100-X} Mg_x/Si(111) Thin Films

T. Chihi, M. Fatmi, B. Barka, S.I. Ahmed, F. Sahnoune

PII: S2211-3797(19)30933-7
DOI: https://doi.org/10.1016/j.rinp.2019.102417
Article Number: 102417
Reference: RINP 102417

To appear in: *Results in Physics*

Received Date: 24 March 2019
Revised Date: 1 June 2019
Accepted Date: 1 June 2019

Please cite this article as: Chihi, T., Fatmi, M., Barka, B., Ahmed, S.I., Sahnoune, F., Structural And Electrical Properties Of Al_{100-X} Mg_x/Si(111) Thin Films, *Results in Physics* (2019), doi: https://doi.org/10.1016/j.rinp.2019.102417

Structural And Electrical Properties Of $Al_{100-X}Mg_x$/Si(111) Thin Films

T. Chihi[1] , M. Fatmi[1,*], B. Barka [1], S. I. Ahmed[2,3], F. Sahnoune[1,4]

[1]Research Unit on Emerging Materials (RUEM), University Ferhat Abbas of Setif 19000, Algeria

[2]Physics Department, Faculty of Sciences, Taif University, Saudi Arabia

[3]Physics department, Ain Shams Univiersity, Cairo, Egypt

[4]Physics Department, Faculty of Sciences, M'sila Universit, Algeria

* Corresponding author: fatmimessaoud@yahoo.fr

Abstract

Morphological and electrical properties of AlMg thin films and the impact of the elaboration conditions on their quality are investigated. For this purpose, thin layers of AlMg of different Mg content were deposited by vacuum evaporation on a monocrystalline silicon substrate in the MECA2000 evaporator. The properties were studied by the X-ray diffraction technique (XRD), XRF, the optical and mechanical profilometer and the four-probe method. The interpretation of the X-ray diffraction spectra allowed us, among other things, to affirm that the films are poly-crystalline with β and δ phases. Generally, the lattice parameter of the Al-Mg samples was slightly higher compared to the bulk one a_{massif}. As a result, our samples show a general increase in grain size as the thickness increases. Observations with optical profilometry, we have established that the surface is of dense appearance with presence of many grains. The results of the measurement of the roughness show increased values with the increase of x at. % Mg whose maximum is at 190 nm corresponding to a x at.% Mg of 97.

As for the electrical measurements, they report a maximum resistivity of 3.6×10^{-3} Ω.cm.

Keywords: thin films; Al-Mg alloys; grains size

1. Introduction

Aluminum, semi-precious metal can be obtained almost pure (Al> 99.99%). Industrial aluminum generally contains about 0.5% impurities, the main ones being iron and silicon. The mechanical properties of unalloyed aluminum are poor. However, these properties can be improved by the addition of alloying elements.

Today, aluminum and its alloys occupy the second place in the industrial construction of different parts after iron. In addition to its wide variety of applications, the low density of aluminum alloys gives it a significant resistance to deformation. It is noted that there are several families of aluminum alloys that differ in their addition elements. In this work, we focus on Al-Mg alloys from the 5000 series, which is known to be lightweight, easy to machine and very strong [**1**].

Since the 1950s, large quantities of Al-Mg alloy have been used in ship structures because of its excellent resistance to corrosion when immersed in seawater [**2**]. The main alloying element in Al-Mg marine alloys is Mg; corrosion resistance increases as the amount of Mg increases [**3**].
The properties of aluminum alloys depend on the metallurgical structure, which in turn depend on the composition, the solidification processes and the deformation processes.
Many additives are added to the aluminum to increase its properties. The main elements increasing the resistance are copper, magnesium, manganese, silicon, and zinc as binary alloys, and Al-Mg-Cu, Al-Mg-Si as ternary alloys and Al-Mg-Cu-Si, Al-Mg-Cu-Zn. All these elements have maximum solubility limits greater than 1.5% and have high diffusion coefficients [**4**]. The application of Al-Mg alloy sheets in different constructions becomes very attractive due to their high strength level, good corrosion resistance and a high potential of weight saving [**5, 6].** Aluminum is used for the manufacture of pipes of all kinds, superstructures of river and the most attractive applications are industrial marine vessels, cables, electrical conductors etc.
Thin films of a given material is the material deposited on a so-called substrate, this deposit has been greatly reduced, in one of their dimensions (thickness). Thin films of Al-Mg are made using several deposition techniques. They can be obtained by operating in the liquid phase or in the vapor phase and by physical or chemical processes. W.A. Soer *et al* **[7]** studied the effects of solute Mg on grain boundary and dislocation dynamics during nanoindentation of Al–Mg thin films, and concluded that solute Mg effectively pins high-angle grain boundaries. H.Ohkubo *et al*. **[8]** observed that in Al–Mg thin films deformed at room temperature, a large number of stacking fault tetrahedra (sft) and a large number of dotted defects (possibly sft) were observed.
L.Pranevicius *et al*. **[9]** studied the behaviors of hydrogen in Al, Mg and MgAl thin films on stainless steel substrate were investigated in this work.
In this study we have focused on the observations of Al-Mg alloys, probing the influence of Mg content on grain size, stress, resistivity and roughness. The Al-Mg phase diagram characterized by the low miscibility of Al and Mg, the maximum miscibility of Mg in solid aluminum is of the order of 17.4% by weight at 450 ° C. The latter decreases to 12.4% Al in solid magnesium by weight at 437 ° C. Ohno *et al*. [**10**] Observed that the solidification of the alloy begins with the

crystallization of the primary phase α-Al. As well as the liquid is enriched in magnesium during the growth of the solid phase [**11**]. The possibility of formation of the intermetallic phases (Al_3Mg_2 and $Al_{12}Mg_{17}$) at (37 and 67% by weight Mg) at low temperatures (450 and 437 ° C) [**12**].

2. Experimental procedures

The material Al-Mg to be characterized is deposited as a thin film onto a Si substrate. The thin layers of $Al_{100-x}Mg_x$ ($0 < x < 100$) have been coevaporated onto Si (111) under vacuum, with Joule heating using an ALCATEL MECA 2000 brand evaporator. In this experiment five films were made. Before the development, contact between the substrates and the hands or any foreign body is avoided in order to minimize the contaminations, the base pressure was $P = 10^{-4}$ mbar, then make the secondary vacuum with the oil diffusion pump until the needle Penning gauge indicates a pressure $P = 3.10^{-6}$ mbar during one day. The crystal structure and microstructure were studied with a Philips X-Pert Pro diffractometer in θ-2θ mode of the Bragg- Brentano geometry, using CuK_α radiation. X-ray diffractograms of the films are recorded in the range of the diffraction angle 2θ: 5°-80° in steps for 0.02 and a counting time of 0.5 s per step.

3. Results and discussions

In **Fig. 1**, the XRD patterns for the $Al_{100-x}Mg_x$/Si(111) thin films with Mg percentage x= 31%, 32%, 50%, 52% and 97% are presented. All the spectra show two intense peaks attributed to the planes Si(111) and Si(222) located at 2θ=28.48° and 58.95°, respectively. This is a direct consequence since a the Si substrate is oriented in the [111] direction has been used.

The two peaks of the Si substrate which belong to the JCPDS file # 01-77-2111, as shown in **Fig. 2**. Beside this, the spectra show Bragg peaks with indices (220), (321) of the cubic γ -$Al_{12}Mg_{17}$ phase corresponding to JCPDS file # 01-73-1148 card, and (533), (711) Bragg peaks corresponding to cubic β-Al_3Mg_2 phases with the JCPDS file # 00-29-0048. Moreover, there are two peaks corresponding to (202), (113) of MgO_4 (JCPDS file # 00-27-0759) and (012) of the Al_2O_3 (JCPDS file # 01-83-2081). It worth noting that, with increasing Magnesium new peaks appear to be diffracted in the patterns of Al-52.97% Mg located at $2\theta = 11.8°$ and another peak at 72.9° from the γ -$Al_{12}Mg_{17}$ phase. Generally, one notes that if the content of magnesium increases, the intensity of the peaks diffracted increase as well. The lattice parameter is computed according to the most intense peak, i.e. $a_\gamma = \sqrt{2}d_{220}$ for γ bcc phase, and $a_\beta = \sqrt{3}d_{933}$ for β AlMg fcc phase; d_{hkl} is the interplanar distance between (hkl) planes. The phase γ structured to

cubic centered bcc with a = 10.5438 Å and β cubic face-centered with a = 28.2390 Å. As shown in **Fig. 3**, the addition of magnesium to aluminum makes the lattice parameter a of the β phase to increase from 28.39 Å to 28.46 Å. For low concentrations, the lattice parameter (31%Mg, 32 %Mg) decreases and then increases, especially for high concentrations (96%Mg). It is worth noting the existence of the two phases β and γ for the values of x = 50% and 52%. Grain boundary motion in metals typically occurs at elevated temperatures, and is driven by a free energy gradient across the boundary, the boundary mobility is greatly reduced by the addition of solutes [**13**]. We calculated the average crystallite size, which is the length of the crystal in the direction of the d spacing, using Scherrer's formula [**14**]:

$$D = \frac{0.9\lambda}{B\cos\theta}$$

where λ is the X-ray wavelength (1.5406 Å), **B** is the full width at half maximum and **θ** is the Bragg diffraction angle. Scherrer's formula teaches that peak broadening is proportional to the inverse of the crystallite size.

The average crystallite size of fcc β -phase thin films decreases when x at. % Mg increase. The results related to XRD measurement are summarized in **Table 1**. We can say that the size of the beta phase varies inversely with that of the gamma phase**,** and that the size of the gamma phase is almost greater than that of the beta phase, for all the concentrations of magnesium studied, especially in the intermediate range (50-52) % Mg, in this interval, betta decreases slowly while gamma increases strongly, because this interval is near to the pure gamma phase, see **Fig. 4**.

Table.1 expresses the variation of the mid-height width, grain size, and the most intense peak area β- (933) in each spectrum. The micro-deformation or stress can be evaluated according to the Stokes-Wilson relationship:

$$\boldsymbol{\varepsilon\ (\%) = \frac{\beta}{(4\tan\theta)}}$$

Stresses (stress) in thin and multilayer layers have three main origins: residual stresses (intrinsic and thermal) and mechanical stresses. The intrinsic stresses are distinguished from the thermal stresses in that they are the stresses present at the deposition temperature. The intrinsic constraints are due to the enlargement of grains, the annihilation of defects (vacant sites), phase change, etc.

If the grain size decreases, the number of grain joints (they are zones of discontinuity and contain a very high density of impurities and crystalline defects) increases, the mobility decreases, the electronic displacement becomes more difficult so the resistivity increases, so we say that a fine-grained material is more electrically resistant.

Fig. 5 shows the variations of the internal stress rate ε % as a function of x at. % Mg for β fcc and γ bcc- phases. Comparison of **Fig. 3** and **Fig. 4** shows that the crystallite size D and the internal strain rate ε evolution *vs*. the magnesium percentage x are inversely proportional. If we want to talk about the residual stress, the grain size and the residual stress are connected to each other, by the fact that, as in our crystallites or for β fcc and γ bcc- phases, the grain size decreases (increases) when the magnesium percentage increases (decreases), that is, the density of the grain boundaries increases (decreases), so planar defects increase and the resistivity increases.

Fig. 6 shows the surface topography of AlMg film observed by means of optical plofilometry. It is observed that the surface morphology presents considerable surface roughness a granular with a regular grain size, we can also observe some ones that are bigger.

The root mean square (rms) roughness has been measured for all samples. The evolution of roughness (rms) as a function of x at. % Mg is presented in **Fig. 7**. We can see that most of the films are rough, the roughness increase with x at. % Mg. Because solutes generally segregate more strongly to high-angle boundaries [**15]** the roughness rms increase with x at. % Mg. The electrical resistivity is calculated as a reciprocal value of conductivity. **Fig.8.** shows the variation of the electrical resistivity which increases with the percentage % Mg. This increase is divided into two parts, the first shows a gradual increase from $3.6.10^{-5}$ Ω.cm to $7.1.10^{-5}$ Ω.cm, when the thickness varies from 148 nm to 152 nm, and the second presents a monotonic increase of the resistivity up to its maximum value of $3.6.10^{-5}$ Ω.cm for a thickness of 454 nm.

4. Conclusion

The object of our study is the experimental study of some physical properties of AlMg alloy in thin layers. To understand the effect of the magnesium content as an additive element in the aluminum alloy, the films were deposited by vacuum evaporation on a directional silicon substrate [111].

The thicknesses of our samples are between 148 nm and 454 nm, and grow with the increase in magnesium in percent which varies between 31% at and 97% at.

The diffractograms correspond to the X-ray study of AlMg films (Al-31, 32, 50, 52, 97% at Mg). The temperature of the deposit is 450 ° C allows to obtain a better crystallization cc and cfc phases ɣ and β respectively, these spectra show that all samples are polycrystalline with different diffraction planes β peaks (211),(220),(640),(653) et δ de pics (620),(933),(880),(12 22), (17 53) respectively, there are new peaks refracted in the Al-52, 97% Mg spectra of the δ: δ (110), δ (811) phase.

The grains size evolution as a function of the thickness of the AlMg films deposited on the Si substrate has an overall decrease with the increase in the thickness of the films. On the other hand, we also noted the growth of the microdeformation with the increase of the thickness for all the samples. The optical profilometer study of the surface morphology of the AlMg samples provides insight into the effect of magnesium content and thickness on the roughness of the film surface. As the thickness increases, the roughness increases. The electrical characterization leads to low values of the resistivity, it increases with increasing thickness. The lowest recorded value of the electrical resistivity is 3.6×10^{-5} Ω.cm, for a thickness of 148 nm. However, the largest recorded value of the electrical resistivity is 3.6×10^{-3} Ω · cm for a thickness of 454 nm.

However, this work concerning AlMg films is old for massive and sheet metal, but it is new for thin films especially of physical study.

References

[1] Sanders R.E., J. H. Industrial development of non-heat treatable aluminum alloys. Mater. Forum. (2004).

[2] Sensharma P., C. M. SSC-4 Effect of Welded Properties on Aluminum Structures. Ship Structure Committee. Washington, DC, USA. (2010).

[3] Picu R.C., V. G. Strain rate sensitivity of the commercial aluminum alloy AA5182-O. Mater. Sci. Eng. A. (2005).

[4] Habashi, F. Alloys: Preparation, Properties, Applications. Wiley-Vichy. (1998).

[5] Sanders Jr., R.E., Hollinshead, P.A., Simielli, E.A.: Mater. Forum 28, 53–64 (2004).

[6] Kobayashi, K., Koga, S., Hino, M.: Conf. Proc. 1st Japan International SAMPE Symposium, pp. 59–64 (1989).

[7] W.A. Soer, J.Th.M. De Hosson, A.M. Minor, J.W. Morris Jr., E.A. Stach, Acta Materialia 52 (2004) 5783–5790

[8] H.Ohkubo, Y.Shimomura, I.Mukouda, K.Sugio, M.Kiritani, Formation of vacancy clusters in deformed thin films of Al–Mg and Al–Cu dilute alloys, Materials Science and Engineering: A, Volume 350, Issues 1–2, 15 June 2003, Pages 30-36

[9] L.Pranevicius, D.Milcius, L.L.Pranevicius, G.Thomas, Plasma hydrogenation of Al, Mg and MgAl films under high-flux ion irradiation at elevated temperature, Journal of Alloys and Compounds, Volume 373, Issues 1–2, 30 June 2004, Pages 9-15

[10] L. L. Rokhlin, 1. N. Dobatkina ALUMINIUM ALLOYSVol. (2004).

[11] OHNO, A. The Solidification of Metals. Tokyo, Japan,. (1976).

[12] Marius, T. C. Maîtrise des interfaces hétérogènes lors d'une opération de soudo-brasage : application au couple aluminium – magnésium. UNIVERSITE DE BOURGOGNE POLITEHNICA TIMISOARA (Roumanie). (2012, octobre).

[13] Lucke K, Detert K,Acta Metall 1957;5;628.

[14] B. D. Cullity, Elements of X-ray Diffraction, Addison-Wesley, 1978, 102.

[15] Sutton AP, Balluffi RW. Interfaces in crystalline solids, Oxford: Clarendon Press; 1995.

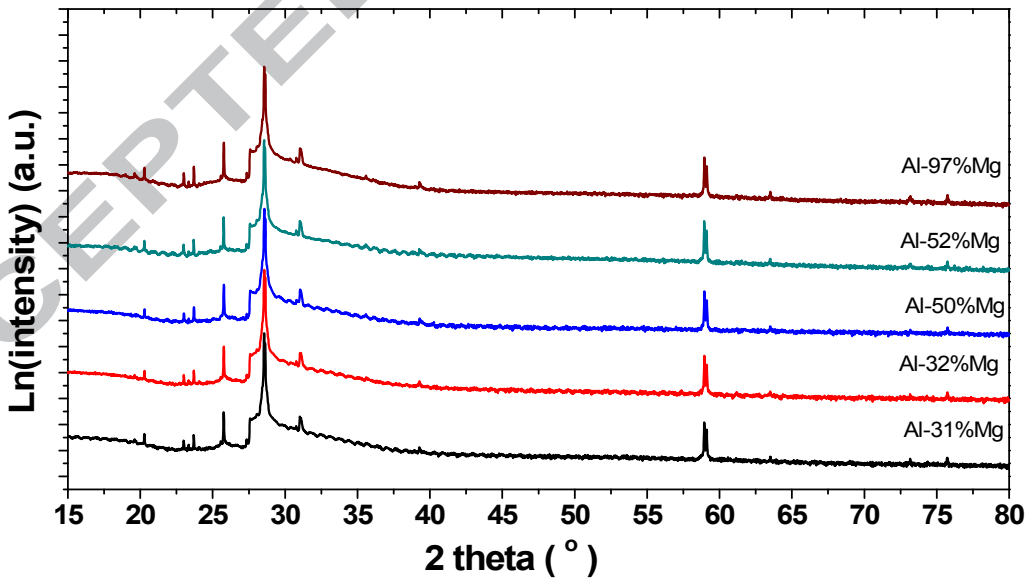

Fig. 1. The XRD patterns of the Al-x%Mg/Si(111) films. Note, the logarithm of the diffracted intensity is plotted versus the diffraction angle 2θ.

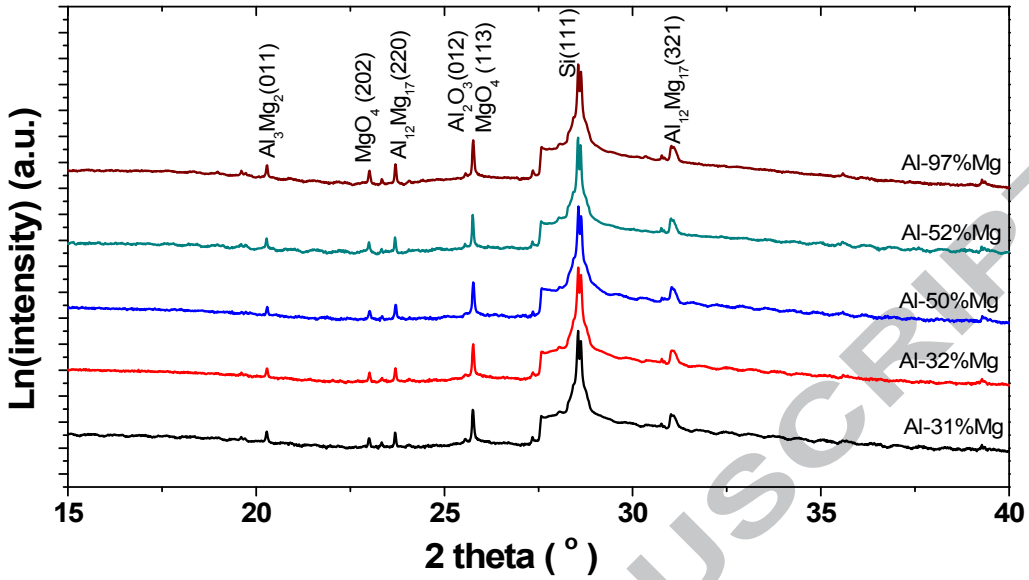

Fig. 2. The XRD patterns of the Al-x%Mg/Si(111) films.

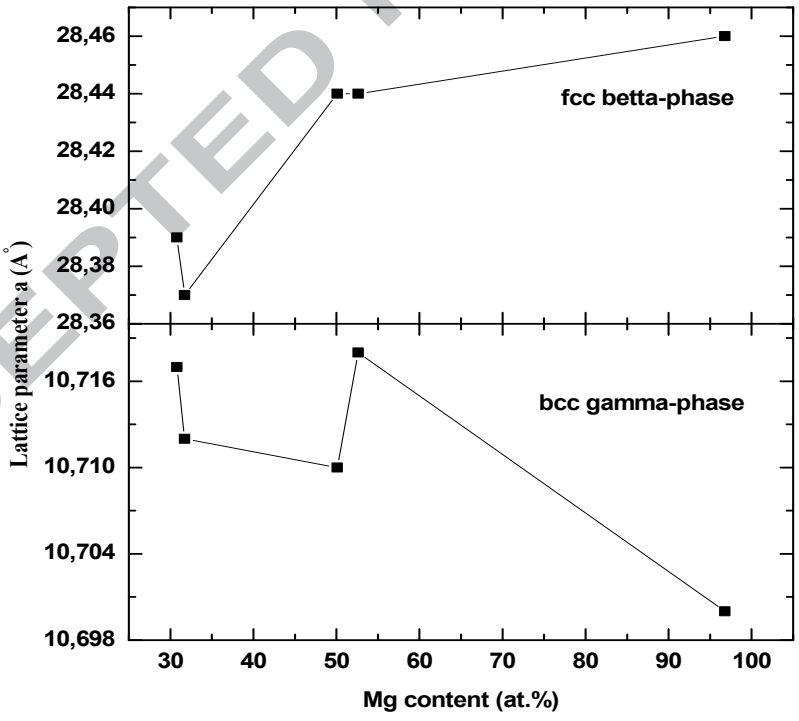

Fig. 3. Lattice parameter *a* as a function of x at. % Mg for β-fcc and γ- bcc- phases.

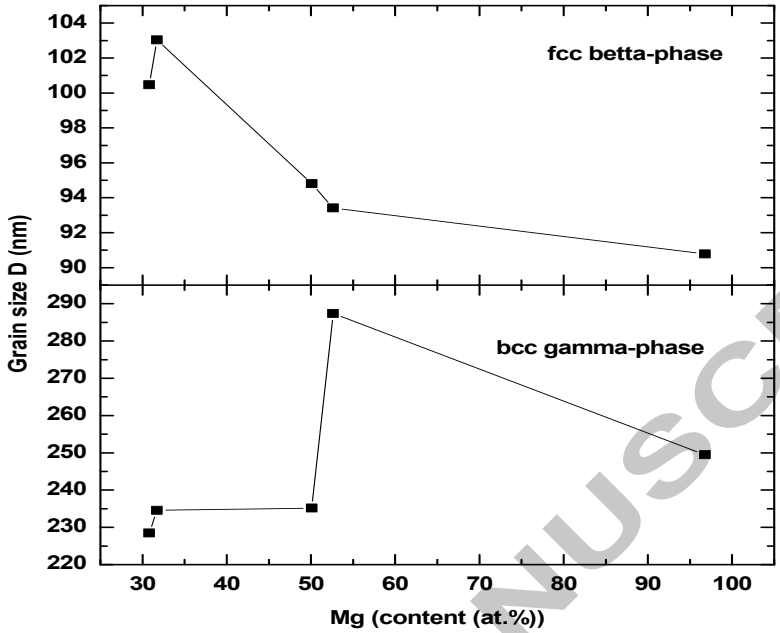

Fig. 4. Grain size D as a function of x at. % Mg for β-fcc and γ- bcc- phases.

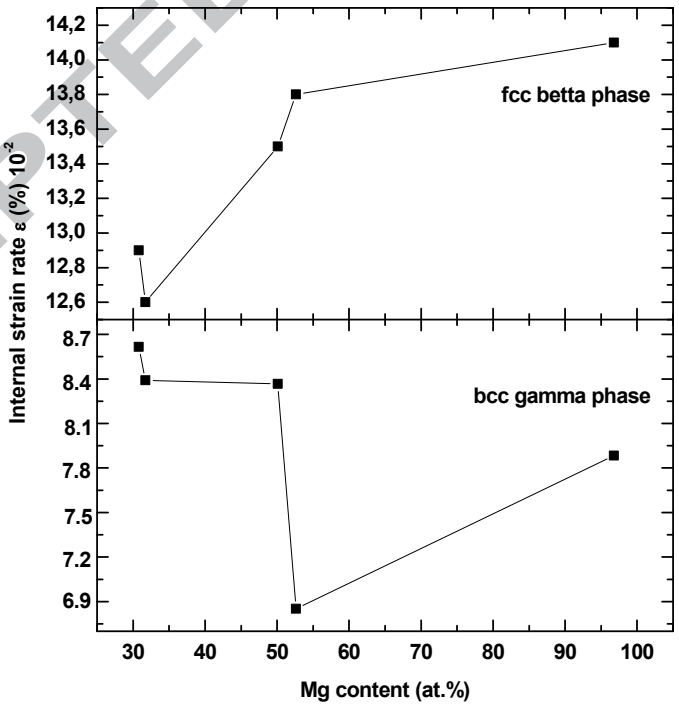

Fig. 5. Internal stress rate as a function of x at. % Mg for β-fcc and γ- bcc- phases.

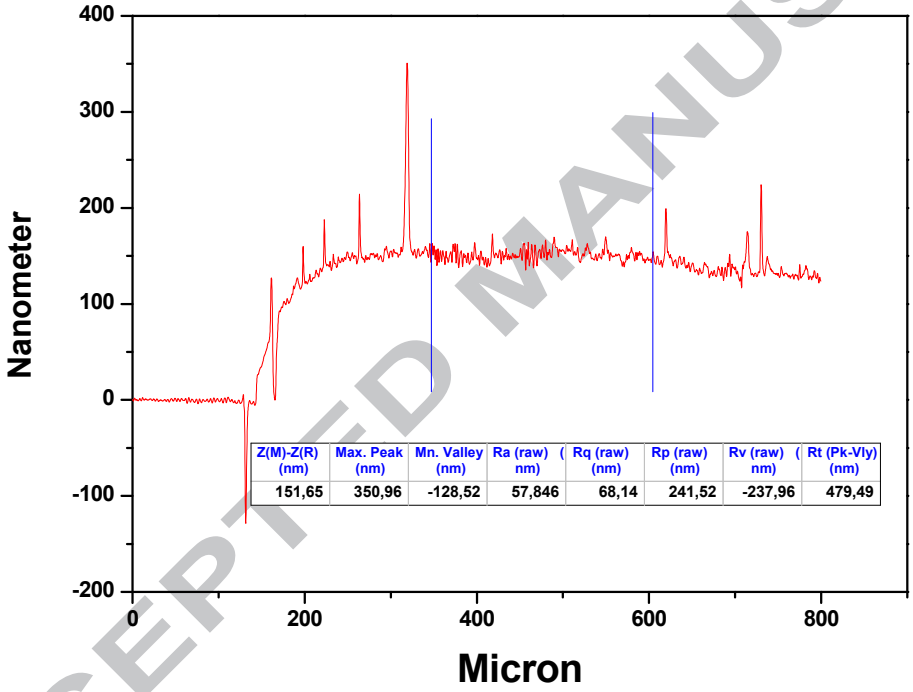

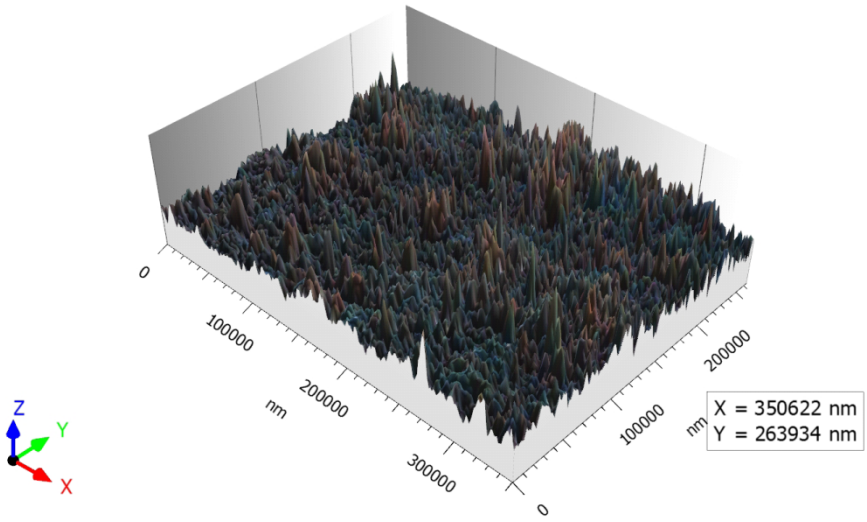

Fig. 6. A surface topography profile measurements and optical profilometry of Al-Mg thin films.

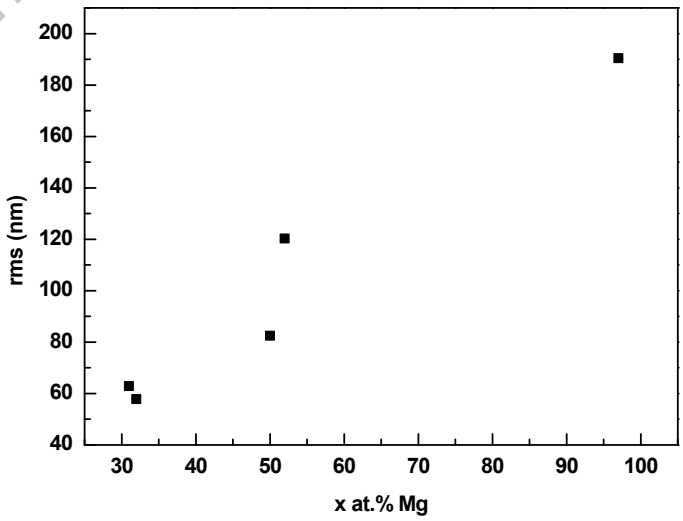

Fig. 7. The evolution of roughness rms as a function of x at.% Mg.

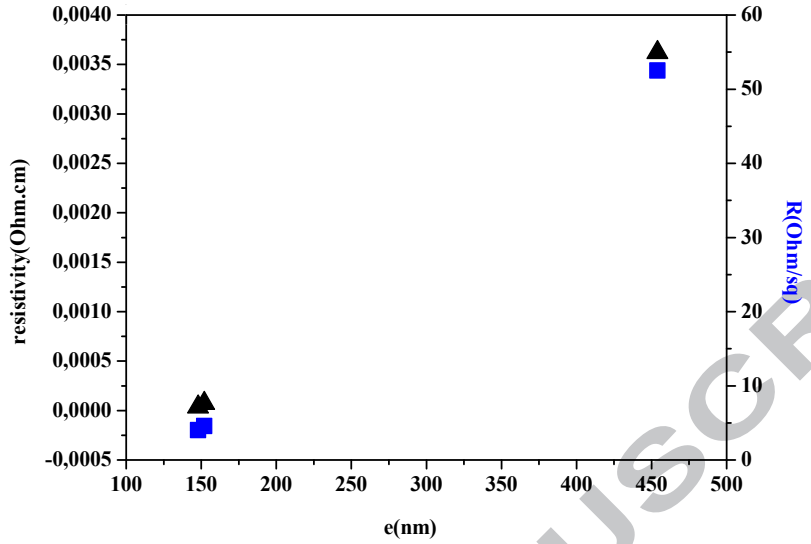

Fig. 8. Resistivity values as a function of film thickness.

Table.1. Width at half height, grain size and peak area of β- (933).

x at.% Mg	31	32	50	52	97
D (nm)	100,46	103,03	94,80	93,41	90,78
A (nm^2)	203,90	182,24	211,34	315,14	525,76